# Use of Isosbestic Points for Determination of Quantum Efficiency in Transient Absorption Spectroscopy

**Yanong Han and Lee H. Spangler***

*Department of Chemistry, Montana State University, Bozeman, Montana 59717*

*Received: October 4, 2001*

Isosbestic points in the transient absorption spectrum for an intermolecular photoinduced electron-transfer system (PET) (bis-(diphenylamino)diphenylbutadiene plus $C_{70}$ in dilute solutions) are observed. An analytical treatment of these points indicate that they are a measure of the quantum efficiency for the PET process. Variation of parameters that affect PET quantum efficiency, such as solvent polarity and photoinitiator lifetime, result in predicted frequency shifts of the isosbestic point. Comparison to established methods of determination of quantum efficiency indicates that the method is quantitatively reliable as well as qualitatively useful. Application of the methodology to other systems is discussed.

## 1. Introduction

Transient absorption methods have proven to be powerful techniques in tracking photophysical and photochemical dynamics. In a number of published studies involving photoinduced electron transfer (PET),[1−6] excited-state absorption,[7−9] and intersystem crossing,[10] as well as in the PET work presented here, an isosbestic point can be observed for a certain time region in the transient absorption spectrum. In some cases, the existence of this point is cited as evidence that there is an interdependence of the two species involved in the absorption at the isosbestic point (IP), but we have not seen a quantitative treatment of isosbestic points in time-resolved data.[11] (We have become aware of an analytical but not quantitative treatment of an isoemissive point during the preparation of this manuscript.[12]) A straightforward consideration, which follows, indicates that analysis of an IP should yield useful information about quantum efficiencies of the system.

We first consider the most common application of an isosbestic point, a case where two species can be interconverted without loss via other pathways (e.g., protonated and deprotonated forms of a chromophore). If the system starts completely in one form, A, then $OD = \epsilon_A[A]_0 l$ where $\epsilon$ is the molar absorptivity and $l$ is the path length. If a portion of A is converted to B, then the OD of the system is dependent on the concentrations of both species

$$OD = \epsilon_A[A]l + \epsilon_B[B]l \tag{1}$$

If the fraction converted is $x$, then $[B] = x[A]_0$ and $[A] = (1 - x)[A]_0$ and eq 1 becomes

$$OD = \epsilon_A(1 - x)[A]_0 l + \epsilon_B x[A]_0 l \tag{2}$$

At most wavelengths, the OD is dependent on pH because [A] and [B] vary with pH. But if the absorption bands of A and B overlap, there may exist a point where $\epsilon_{A,\lambda} = \epsilon_{B,\lambda}$, and the OD at that given wavelength, $\lambda$, is independent of the pH for all physically meaningful values of $x$ ($x \leq 1$). This results in an isosbestic or isoabsorptive point in the spectrum.

If we now consider a case where the conversion of A to B occurs with an efficiency, $\Phi < 1$, then a reduction in A by an amount $x$ results in formation of $x\Phi$ of B; our absorbance equation would then have the form

$$\begin{aligned} OD &= \epsilon_A[A]l + \epsilon_B[B]l \\ &= \epsilon_A(1 - x)[A]_0 l + \epsilon_B x\Phi[A]_0 l \end{aligned} \tag{3}$$

because $[A] = (1 - x)[A]_0$ and $[B] = x\Phi[A]_0$. In eq 3, constant OD will not occur where $\epsilon_{A,\lambda} = \epsilon_{B,\lambda}$ but will instead be where $\epsilon_{A,\lambda} = \Phi\epsilon_{B,\lambda}$. So, an isosbestic point where the *absorption* of the system is constant still appears; however, it differs from the first case in that it is *not* where the absorption *coefficients* are equal. Rearranging gives

$$\Phi = \frac{\epsilon_{A,\lambda}}{\epsilon_{B,\lambda}} \tag{4}$$

and we see that the ratio of the absorption coefficients at the IP yields the quantum efficiency of the conversion process. What occurs in transient absorption data is more complicated and requires a more detailed treatment (to be presented later), but this conceptually illustrates that there is a relationship between efficiencies and the isosbestic point. Specifically, the work presented here explores use of an IP as a measure of quantum efficiency in photoinduced electron transfer, and we will discuss applicability to other systems.

## 2. Experimental Section

The bis-(diphenylamino)diphenylbutadienes used as electron donors in this study were synthesized by the Charles W. Spangler research group. $C_{70}$, 99.5% purity, was purchased from Aldrich and used without further purification.

All photoinduced absorption (PIA) measurements were performed in solution in 1 cm quartz cuvettes. Solutions were deoxygenated by bubbling Ar gas for 15 min resulting in $^3C_{70}$* lifetimes of 6 $\mu$s (in $C_{70}$ only solutions, without donor present). A 50 W continuous tungsten filament lamp was used as the

* To whom correspondence should be addressed. Tel: (406) 994-4399. E-mail: lspangler@chemistry.montana.edu.

10.1021/jp013717x CCC: $22.00 
Published on Web 02/07/2002

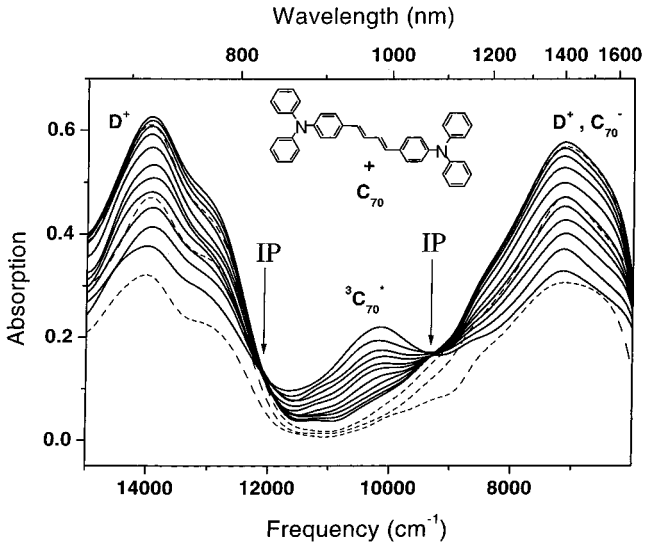


**Figure 1.** The transient absorption spectrum due to photoinduced electron transfer of 0.20 mM bis-(diphenylamino)diphenylbutadiene and 0.10 mM $C_{70}$ in benzonitrile. Two isosbestic points are observed in the 0.5−2.0 $\mu$s time region (solid lines), which disappear at longer times as illustrated by the dashed lines (at 5, 10, and 20 $\mu$s).

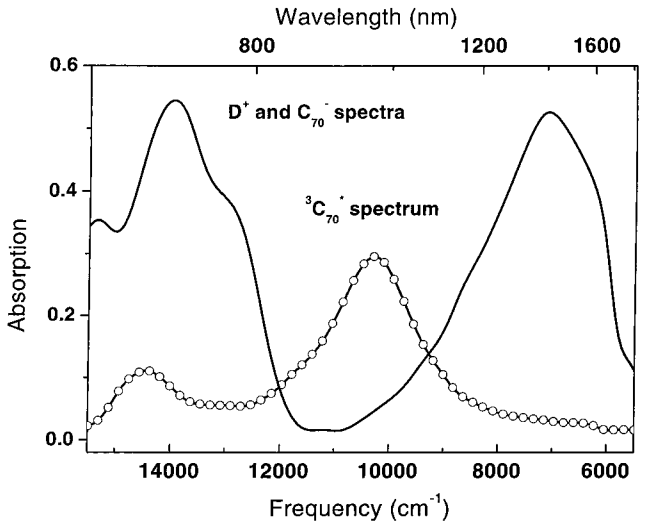


**Figure 2.** Spectral components of Figure 1. The solid line shows spectra from the $D^+$ and $C_{70}^-$ ions obtained from the transient absorption at long times after $^3C_{70}$* has completely decayed. The $^3C_{70}$* spectrum (line with circles) was obtained from a $C_{70}$ benzonitrile solution without donor.

broadband probe source and was focused with F/5 optics through the center of the cuvette. A Coherent Infinity Nd:YAG laser frequency doubled to 532 nm was used as a pump (typically 2−3 mJ/pulse) in a quasi-coaxial geometry with the probe light. After passing through the sample, the broadband light was refocused on an aperture where only the middle 20% of the laser spatial profile was sampled to reduce excitation gradients and their resulting problems, such as thermal lensing.

The light was then directed into a Bruker IFS 88 step-scan interferometer to acquire the time and frequency resolved PIA spectrum. An InSb detector and broad-band beam splitter were used to measure the transient spectrum from 15 798 to 2000 $cm^{-1}$. The typical three-dimensional spectra produced consisted of 400 traces with 300 $cm^{-1}$ spectral resolution and 50 ns temporal resolution.

### 3. Results and Interpretation

**Isosbestic Point Observation and Analysis.** The transient absorption spectra of 0.10 mM $C_{70}$ and 0.20 mM bis-(diphenylamino)diphenylbutadiene (D) in benzonitrile (BN) are shown in Figure 1, where the measured value is a ΔOD caused by the laser pump. At early times, the photoinduced absorption peak centered at 10 200 $cm^{-1}$ is due to $^3C_{70}$ absorption.[13−15] As this peak decays, a very broad transition grows in the near-IR with a peak at 13 950 $cm^{-1}$ and a shoulder at 12 900 $cm^{-1}$, which can be attributed to $D^+$, the singly charged bis-(diphenylamino)-diphenylbutadiene donor cation that has been identified in previous work. A 7160 $cm^{-1}$ band is primarily due to the intervalence transition of $D^+$. Treatment of this compound in solution with $SbCl_5$ to chemically oxidize it produces the same $D^+$ transitions. Also contributing to the spectrum is the well-known $C_{70}^-$ absorption band (7200 $cm^{-1}$)[16], which appears highly overlapped with the broad intervalence band of $D^+$.

Inspection of the transient absorption spectrum at early times (0.3−2 $\mu$s) reveals two regions, near 12 000 and 9000 $cm^{-1}$, that have the same appearance as an isosbestic point. The existence of this point is evidence of the interdependence of the concentrations of the photoinduced species. These two points occur because the $^3C_{70}$* absorption lies between, and overlaps, the two absorption regions of the donor cation (Figure 2). The IP regions occur in the time-resolved spectrum, so for these points over the time that they are observable, $(d(\Delta OD)/dt)_{\lambda=iso} = 0$. To see how this point might be useful in determination of quantum efficiencies in dynamical processes, we have to consider the species that contribute to the ΔOD observed and their time dependence.

The PIA spectrum is the difference between absorbance of the photopumped sample and that of the unpumped sample given by

$$\begin{aligned}\Delta OD &= \ln(I_{unpump}/I_0) - \ln(I_{pump}/I_0) \\ &= \{\epsilon_A([A] - [A]_0) + \epsilon_D([D] - [D]_0) + \epsilon_{A^*}([A^*] - \\ &\quad [A^*]_0) + \epsilon_{A^-}([A^-] - [A^-]_0) + \epsilon_{D^+}([D^+] - \\ &\quad [D^+]_0)\}l \quad (5)\end{aligned}$$

where, generically, $[Y]_0$ is the concentration of Y in the unpumped condition. Only the ground-state neutral donor and acceptor are present before excitation, so $[A^*]_0 = [A^-]_0 = [D^+]_0 = 0$ and the path length, $l$, is 1 cm. With these simplifications and taking into account that we are looking at the *temporal* behavior of this difference spectrum, we arrive at

$$\begin{aligned}\frac{d(\Delta OD)}{dt} &= \epsilon_A\frac{d([A] - [A]_0)}{dt} + \epsilon_D\frac{d([D] - [D]_0)}{dt} + \\ &\quad \epsilon_{A^*}\frac{d[A^*]}{dt} + \epsilon_{A^-}\frac{d[A^-]}{dt} + \epsilon_{D^+}\frac{d[D^+]}{dt} \quad (6)\end{aligned}$$

The first two terms represent bleaching of the ground state of the initial species, and the last three terms are new absorptions caused by photoinduced species. In the wavelength region where the 12 000 $cm^{-1}$ isosbestic point is observed, there is no ground-state absorption due to either the donor or acceptor, and the acceptor anion also does not absorb. Thus, for this point, $\epsilon_{A,\lambda} = \epsilon_{D,\lambda} = \epsilon_{A^-,\lambda} = 0$, and eq 6 simplifies to

$$\frac{d(\Delta OD)_\lambda}{dt} = \epsilon_{A^*,\lambda}\frac{d[A^*]}{dt} + \epsilon_{D^+,\lambda}\frac{d[D^+]}{dt} \quad (7)$$

**SCHEME 1**

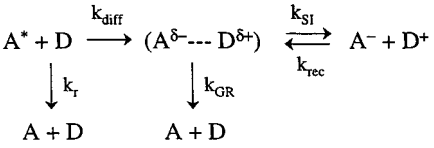


The decay of the A* signal and the rise of the $D^+$ signal occur with the same rate constant indicating a diffusion-limited process for which the mechanism shown in Scheme 1 is appropriate. As shown in previous work,[17] application of the steady-state approximation to the intermediate results in

$$\frac{d[D^+]}{dt} = k_{diff}\Phi_{SI}[A^*][D] - k_{rec}[A^-][D^+](1 - \Phi_{SI}) \quad (8)$$

for the cation behavior, where $\Phi_{SI} = k_{SI}/(k_{SI} + k_{GR})$ is the quantum efficiency for formation of solvated ions from the intermediate. The time dependence of the photoprepared species can be obtained by inspection of the mechanism and is

$$\frac{d[A^*]}{dt} = -k_r[A^*] - k_{diff}[A^*][D] \quad (9)$$

Substitution into eq 7 yields

$$\frac{d(\Delta OD)_\lambda}{dt} = \epsilon_{A^*,\lambda}\{-k_r[A^*] - k_{diff}[A^*][D]\} + \epsilon_{D^+,\lambda}\{k_{diff}\Phi_{SI}[A^*][D] + k_{rec}(1 - \Phi_{SI})[A^-][D^+]\} \quad (10)$$

As stated previously, at the isosbestic wavelength, over the time duration when the isosbestic point is observed, the delta absorption does not change,

$$\left[\frac{d(\Delta OD)_\lambda}{dt}\right]_{t=t_{isos}} = 0 \quad (11)$$

making the left-hand side of eq 10 equal to zero. Now, we divide by $\epsilon_{D^+,\lambda}(k_r[A^*] + k_{diff}[A^*][D])$

$$0 = -\frac{\epsilon_{A^*,\lambda}}{\epsilon_{D^+,\lambda}} + \left\{\frac{k_{diff}[D]}{k_{diff}[D] + k_r}\Phi_{SI} + \frac{k_{rec}(1 - \Phi_{SI})}{k_{diff}[D] + k_r}\frac{[A^-][D^+]}{[A^*]}\right\} \quad (12)$$

or, because $k_{diff}[D]/(k_{diff}[D] + k_r)$ is the quantum efficiency for quenching, $\Phi_Q$, and $\Phi_Q\Phi_{SI} = \Phi$,

$$0 = -\frac{\epsilon_{A^*,\lambda}}{\epsilon_{D^+,\lambda}} + \left\{\Phi + \frac{k_{rec}(1 - \Phi_{SI})}{k_{diff} + k_r/[D]}\frac{[A^-][D^+]}{[A^*][D]}\right\} \quad (13)$$

Additionally, the isosbestic point occurs at early time when $[A^*][D] \gg [A^-][D^+]$, causing $\Phi$ to dominate the bracketed term in eq 13. The result is what we anticipated conceptually in the Introduction,

$$\frac{\epsilon_{A^*,\lambda}}{\epsilon_{D^+,\lambda}} = \Phi \quad (\text{at } t = \text{early, when isosbestic point is observable}) \quad (14)$$

The extinction coefficients for $^3C_{70}$* and $C_{70}^-$, are available from the literature. The extinction coefficient for the donor cation was obtained in a previous study where $C_{60}$ was used as an acceptor by comparison of the $D^+$ absorption with the well-known $C_{60}^-$ absorption. The absorption spectra of $^3C_{70}$* and the two ions are shown in Figure 2. Evaluation of the data in Figure 1, $C_{70}$ and bis-(diphenylamino)diphenylbutadiene in BN for the lower frequency IP, yields $\nu_{isos} = 9300\ cm^{-1}$, where $\epsilon_{A^*,\lambda}/\epsilon_{D^+,\lambda} = \Phi = 29\%$. Values obtained for the higher frequency isosbestic point are provided in Table 1, and the quantum efficiency obtained, $\Phi = 28\%$, is in good agreement with the lower frequency point.

**TABLE 1: Isosbestic Points, Quantum Efficiencies for Electron Transfer via Four Methods (see text), and Parameters Used for Their Determination for a Solution of 0.20 mM Bis-(diphenylamino)diphenylbutadiene and 0.10 mM $C_{70}$ in Benzonitrile**

| parameter | value | Φ |
|---|---|---|
| isos pt 1 freq | 9300 $cm^{-1}$ | |
| $\epsilon_{^3C_{70}}$ at 9300 $cm^{-1}$ | 3118 $M^{-1}\,cm^{-1}$ | 0.29 |
| $\epsilon_{D^+/C_{70}^-}$ at 9300 $cm^{-1}$ | 10 886 $M^{-1}\,cm^{-1}$ | |
| isos pt 2 freq | 12 000 $cm^{-1}$ | |
| $\epsilon_{^3C_{70}}$ at 12 000 $cm^{-1}$ | 1904 $M^{-1}\,cm^{-1}$ | 0.28 |
| $\epsilon_{D^+}$ at 12 000 $cm^{-1}$ | 6826 $M^{-1}\,cm^{-1}$ | |
| $[D^+]_{corrected\ max}$ | 16.1 $\mu$M | 0.30 |
| $[^3C_{70}]_{max}$ | 54.6 $\mu$M | |
| $[D^+]_{experimental\ max}$ | 12.5 $\mu$M | 0.23 |
| slope of $d[D^+]/dt$ vs $[^3C_{70}]$ | 0.385 $\mu s^{-1}$ | 0.30 |
| $k_{decay}$ for $^3C_{70}$ | 1.35 $\mu s^{-1}$ | |

**Kinetic Analysis.** To demonstrate that the isosbestic point frequency is a quantitatively reliable measure of quantum efficiency, it is desirable to compare it with quantum efficiencies obtained with other methods. To that end, we performed a kinetic analysis by a method previously published[17] for a system containing the same donor with $C_{60}$ as the photoinitiated acceptor.

The $^3C_{70}$* observed decay rate constant, $k_{decay} = k_r + k_{diff}[D] = k_r + k_Q$, was measured for each solution. Kinetic treatment[17] of the mechanism in Scheme 1 showed that at long times ($t > 5\tau_{decay}$) the donor ion concentration, $[D^+]$, should follow second-order kinetics for recombination according to

$$\frac{1}{[D^+]_t} = \{k_{rec}(1 - \Phi_{SI})\}t + \frac{1}{[D^+]_{t,max}} \quad (\text{corrected for BET}) \quad (15)$$

with a plot of $1/[D^+]$ vs time yielding a slope of $k_{rec}(1 - \Phi_{SI})$, which is an effective back electron-transfer rate constant, $k_{BET}$. The quantity $\Phi_{SI}$ is the quantum efficiency out of the intermediate and is equal to $k_{SI}/(k_{GR} + k_{SI})$. After $k_{BET}$ is determined, the recombination behavior can be subtracted from the $D^+$ temporal behavior to yield a calculated signal that does not decay. It was shown for this corrected signal, and this mechanism, that the donor rise kinetics should follow

$$[D^+]_t = \frac{k_Q}{k_r + k_Q}\Phi_{SI}[A^*]_0\{1 - e^{-(k_r+k_Q)t}\} \quad (\text{corrected to remove BET}) \quad (16)$$

The argument for the exponential rise term is identical to the decay term for the excited acceptor, and the criterion that $\tau_{rise,D^+} = \tau_{decay,A^*}$ for the BET-corrected data is a good test of the overall ET process being diffusion-limited (Figure 3). All solutions investigated here meet that criterion to within 5%.

The BET-corrected data also allow determination of quantum efficiencies in the system via two methods. The first uses a ratio of the maximum concentration of the excited acceptor and the maximum concentration of the donor cation in the BET-

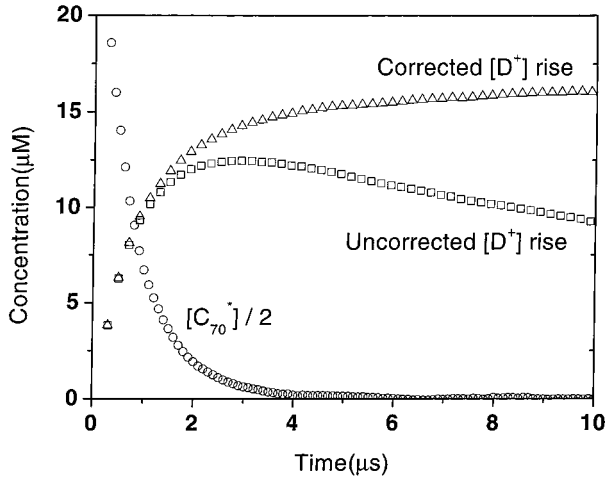


**Figure 3.** Temporal behavior of the $^3C_{70}$* peak (circles, divided by 2) and $D^+$ peak (squares). The third data set (triangles) gives the $D^+$ rise with back electron transfer mathematically removed which provides a more accurate determination of quantum efficiency for the forward electron-transfer process.

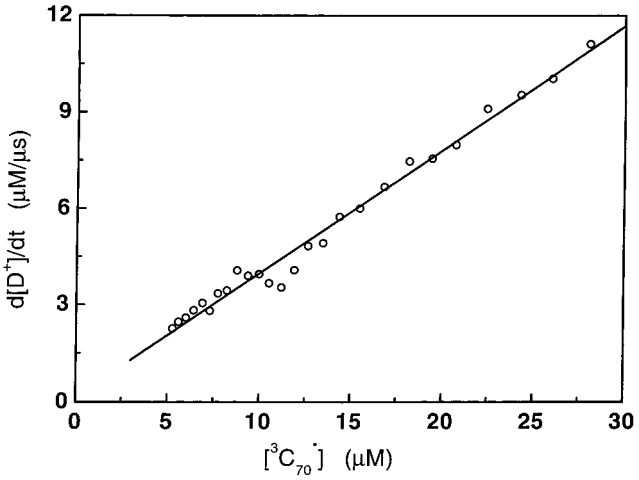


**Figure 4.** A plot of $d[D^+]/dt$ vs $[^3C_{70}^*]$ (circles) with a fit of the slope (line). The slope of this plot is equal to $k_Q\Phi_{SI}$, and division by $k_{decay}$ for $^3C_{70}$* yields the total quantum efficiency, $\Phi$.

corrected data to obtain the overall quantum efficiency.

$$\Phi = \frac{[D^+]_{t,max}}{[A^*]_{max}} \qquad \text{(corrected for BET)} \qquad (17)$$

This treatment was shown to yield an actual quantum efficiency that is a ratio of relevant rate constants given by the equation

$$\Phi = \Phi_Q\Phi_{SI} = \frac{k_{diff}[D]}{k_{diff}[D] + k_r}\frac{k_{SI}}{k_{GR} + k_{SI}} \qquad (18)$$

By contrast, use of the *experimental* maximum ion concentration generates a quantum yield for one specific time—when the ion formation and recombination are balanced.

The second method of determining efficiencies arises from the differential equation governing the temporal behavior of the cation,

$$\frac{d[D^+]}{dt} = k_{diff}\Phi_{SI}[A^*][D] - k_{rec}[A^-][D^+](1 - \Phi_{SI}) \qquad (19)$$

The second term is due to the back electron transfer and mathematically subtracting this results in

$$\frac{d[D^+]}{dt} = k_{diff}\Phi_{SI}[A^*][D] = k_Q\Phi_{SI}[A^*]$$

($D^+$ rise, corrected for BET) (20)

Use of step-scan Fourier transform techniques to acquire the transient absorption spectrum yields very high S/N temporal traces that allow plotting of first-derivative data with very well-defined slopes.[17] Figure 4 is a plot of $d[D^+]/dt$ vs $[^3C_{70}^*]$ with a slope of $k_Q\Phi_{SI} = k_{diff}[D]\Phi_{SI}$. Because the observed $^3C_{70}$* decay is $k_{decay} = k_r + k_{diff}[D]$, division of the first derivative slope by $k_{decay} = k_r + k_{diff}[D]$ yields the total quantum efficiency, $\Phi$, as in eq 18.

Table 1 compares quantum efficiencies obtained via three methods, isosbestic point analysis, corrected maximum value, and first derivative plot. The three methods are in good agreement. To establish the IP as a true measure of quantum efficiency, it is desirable to vary system parameters that have known effects on the quantum efficiency and see whether the point exhibits the correct qualitative and quantitative changes.

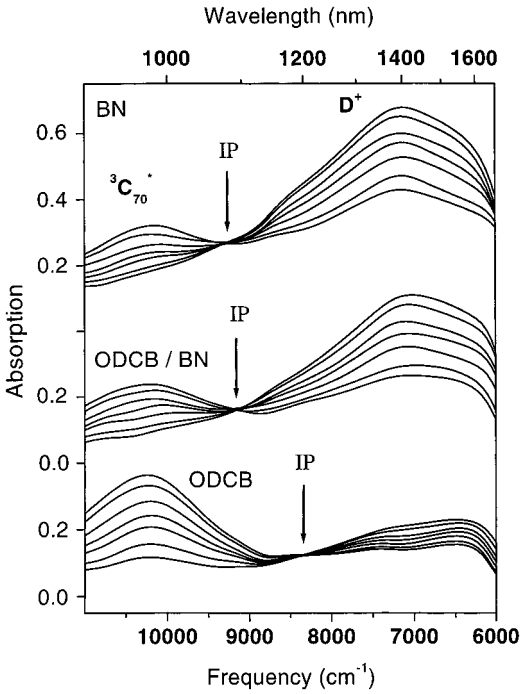


**Figure 5.** The solvent polarity dependence of the isosbestic point (IP) in benzonitrile (top), *o*-dichlorobenzene (bottom), and a 1:1 mixture of the two (middle). A smaller region than Figure 1 is shown so that the IP shift is more discernible. In less-polar solvents (*o*-dichlorobenzene, bottom), the IP is low on the photoinitiated species peak ($^3C_{70}$* at 10 200 $cm^{-1}$). The point shifts higher on the $^3C_{70}$* peak (toward higher frequency) as quantum efficiency increases in more-polar solvents. The difference in efficiency is also apparent in the changes in the relative intensity of the $D^+$ peak compared to the $^3C_{70}$* peak.

**Solvent Effects.** It is well-known that increased solvent polarity improves quantum yield in PET in dilute solutions. Furthermore, in work on the same donor with a closely related acceptor ($C_{60}$), a solvent polarity dependence was demonstrated by using varying mixtures of an *o*-dichlorobenzene/benzonitrile (ODCB/BN) binary solvent.[17] Figure 5 shows the IP behavior in pure ODCB, a 1:1 ODCB/BN mix, and pure BN (in order of increasing polarity). In all cases, the bis-(diphenylamino)-diphenylbutadiene was 0.2 mM and the $C_{70}$ was 0.1 mM with 3 mJ/pulse pump energy at 532 nm used. From eq 14, we expect

**TABLE 2: Effect of Solvent Polarity, Dissolved Oxygen, and Pump Power (Photoinitiator Concentration) on the Isosbestic Point and Quantum Efficiency[a]**

| | | quantum efficiency, Φ | | | |
|---|---|---|---|---|---|
| experimental conditions | isos freq ($cm^{-1}$) | isos | 1st deriv | cor max | exptl max |
| BN solvent | 9300 | 0.29 | 0.30 | 0.30 | 0.23 |
| 1:1 BN/ODCB solvent | 9160 | 0.22 | 0.23 | 0.22 | 0.19 |
| ODCB solvent | 8380 | 0.06 | 0.08 | 0.07 | 0.06 |
| higher [$O_2$], BN solvent | 9000 | 0.16 | 0.15 | 0.16 | 0.15 |
| higher pump power, BN solvent | 9300 | 0.29 | 0.28 | 0.29 | 0.25 |

[a] Values of Φ determined by three other methods provided for comparison.

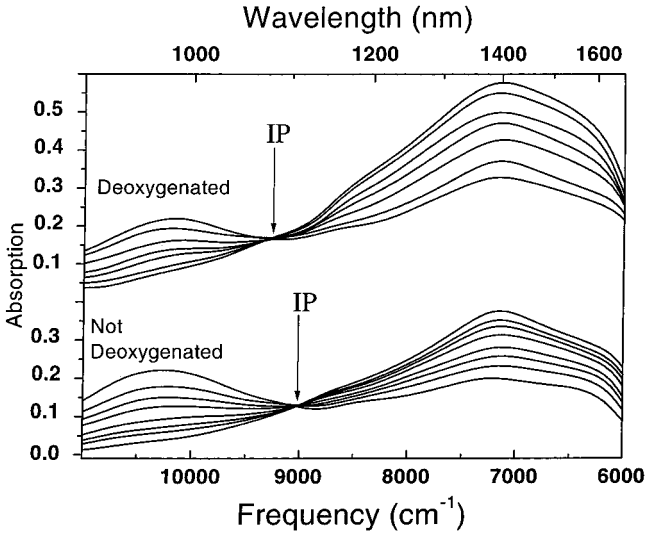


**Figure 6.** The oxygen concentration dependence of the isosbestic point. Presence of oxygen reduces the effective lifetime of the $^3C_{70}$* and causes a reduction of quantum efficiency. Accordingly, the IP shifts lower on the $^3C_{70}$* peak when more oxygen is present (bottom).

the ratio $\epsilon_{A^*,\lambda}/\epsilon_{D^+,\lambda}$ to increase as quantum efficiency increases, and both isosbestic points should shift *higher* up on the $^3C_{70}$* absorption band as the BN fraction increases. Indeed, the correct qualitative behavior is observed. Additionally, determination of efficiencies by the isosbestic point and by the corrected maximum value method yields very good quantitative agreement for all solvent mixtures (Table 2).

**Varying $k_r$.** Changes in solvent polarity effect the $\Phi_{SI}$ component of the quantum efficiency. The other component, $\Phi_Q$, can be addressed by changing the relaxation rate of $^3C_{70}$*. While the intrinsic triplet lifetime cannot be changed, in most solutions, the lifetime is really determined by quenching with dissolved $O_2$, which does not lead to charge transfer. (Deoxygenation by bubbling with Ar or $N_2$ gas typically results in lifetimes of ~6 μs, whereas the actual lifetime appears to be around 2.2 ms as obtained from solutions taken through multiple freeze−thaw cycles).[15] Thus, the effective $k_r$ can be increased by not deoxygenating the solution. Equation 18 shows that this should have the effect of decreasing both $\Phi_Q$ and the total quantum efficiency, Φ. Figure 6 shows PIA spectra with and without deoxygenation. Without deoxygenation, the isosbestic point shifts lower on the $^3C_{70}$* peak indicating the lower quantum efficiency. In addition to displaying the correct qualitative behavior, comparison of the efficiencies determined by the IP and by the established method are in good quantitative agreement.

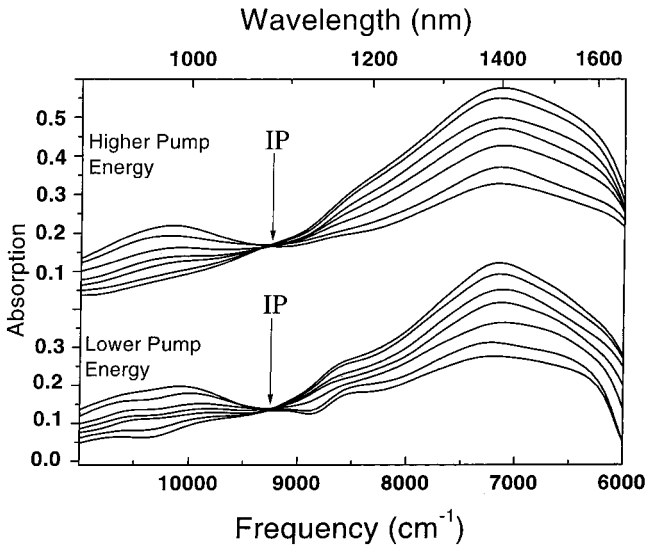


**Figure 7.** The effect of $^3C_{70}$* concentration on the isosbestic point. Higher pump energies (top) result in greater [$^3C_{70}$*], which increases the total amount of ion produced as shown by the larger ion peak at 7200 $cm^{-1}$ (1400 nm), but it does *not* increase the quantum efficiency as illustrated by the lack of frequency shift in the IP.

**Photoinitiator Concentration.** Because the A* concentration does not appear in eq 18, changes in the $^3C_{70}$* concentration produced either by changing [$C_{70}$] or the pump power should have no effect on the quantum efficiency or the isosbestic point frequency. Figure 7 shows data taken for 0.2 mM donor and 0.1 mM $C_{70}$ in BN with two different pulse energies. The difference in pulse energy is evident in the amplitude of the signal because the *amount* of $^3C_{70}$* and $D^+$ produced increases at higher pump power. However, the *efficiency* does not and the isosbestic point exhibits the correct qualitative behavior; it does not shift in frequency.

## 4. Discussion

All of the work presented above demonstrates that the isosbestic point exhibits the correct qualitative and quantitative behavior to be used as a measure of quantum efficiency. It is particularly convenient as a qualitative measure because changes in efficiency can easily be seen by inspection. The quantitative advantages may be less obvious and therefore warrant discussion.

Inspection of Tables 1 and 2 shows that quantum efficiencies determined from the isosbestic point give values closer to the corrected maximum value method than the uncorrected. This and the fact that the point is observed at early times in the conversion process are directly related. Simplification of eq 13 to the working equation $\epsilon_{A^*,\lambda}/\epsilon_{D^+,\lambda} = \Phi$ required that [A*][D] ≫ [$A^-$][$D^+$], which will occur at early times. At later times, [$A^-$] and [$D^+$] concentrations become higher and back electron-transfer becomes significant. This represents a loss of population *after* products are formed, so if not properly treated it will cause an underestimate of the ion formation. This is the reason use of the experimental maximum value for ion concentration does not provide an accurate quantum efficiency for formation of charged states, and we correct for this by first subtracting the back electron transfer (BET) then using the maximum value. The isosbestic point that we measure is providing information about the branching ratio between products and the ground state. The loss in population after product formation due to BET interferes with this ratio, so the isosbestic point is only observed at times when back electron transfer is low (because of low ion

**SCHEME 2**

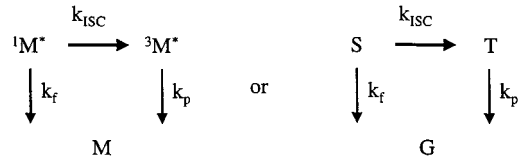


concentration). Thus, in this system, IP determination of quantum efficiency is inherently free of BET interference and should accurately reflect the formation efficiency, as does the corrected maximum value method.

This work focused on transient absorption in a photoinduced electron transfer (PET) system, and the applicability in other systems should be addressed. Obviously, some overlap of absorption features for initial and subsequently formed species must exist for an isosbestic point to be observed. In PET systems, the broad bands and the fact that two products are formed, $D^+$ and $A^-$, mean that this should occur in at least some cases, and we have noticed isosbestic points in PET work in the literature.[1−6] Additionally, PET is not the only dynamical process that should lead to IPs in time-resolved data. For example, consider an excited singlet state that has two relaxation pathways, fluorescence emission to the ground state or efficient intersystem crossing (ISC). The mechanism for this photophysical system is shown in Scheme 2. Such a system would be expected to exhibit an isosbestic point under the following conditions: the photoinduced absorption bands for $^1$M*, and $^3$M* overlap; the fluorescence rate, $k_f$, and intersystem crossing rate, $k_{ISC}$, are similar in magnitude; the phosphorescence emission rate, $k_p$, is slower than both $k_f$ and $k_{ISC}$.

In fact, these conditions exist for $^1C_{60}$* and $^3C_{60}$*, and published picosecond transient absorption spectra do exhibit an isosbestic point.[10] We can easily show the relationship between the observed IP and the quantum efficiency for intersystem crossing, $\Phi_{ISC}$, by following the treatment presented in the previous section. Because both the singlet and triplet PIA bands occur in a spectral region with no ground-state absorption and the unpumped sample contains no excited singlet or triplet, we get

$$\frac{d(\Delta OD)_\lambda}{dt} = \epsilon_{S,\lambda}\frac{d[S]}{dt} + \epsilon_{T,\lambda}\frac{d[T]}{dt} \qquad (21)$$

for the temporal behavior in the relevant spectral region. Here, S denotes the excited singlet and T the excited triplet. From the mechanism, we can write

$$\frac{d[S]}{dt} = -k_f[S] - k_{ISC}[S]$$

$$\frac{d[T]}{dt} = k_{ISC}[S] - k_p[T] \qquad (22)$$

Substituting into eq 21 and recalling that the OD does not change at the isosbestic point yields

$$\frac{d(\Delta OD)_\lambda}{dt} = 0 = \epsilon_{S,\lambda}(-k_f[S] - k_{ISC}[S]) + \epsilon_{T,\lambda}(k_{ISC}[S] - k_p[T]) \qquad (23)$$

If we now divide by $\epsilon_{T,\lambda}(k_f[S] + k_{ISC}[S])$, we get

$$0 = -\frac{\epsilon_{S,\lambda}}{\epsilon_{T,\lambda}} + \left\{\frac{k_{ISC}}{k_{ISC} + k_f} - \frac{k_p[T]}{k_{ISC}[S] + k_f[S]}\right\} \qquad (24)$$

or

$$\frac{\epsilon_{S,\lambda}}{\epsilon_{T,\lambda}} = \left\{\Phi_{ISC} - \frac{k_p[T]}{k_{ISC}[S] + k_f[S]}\right\} \qquad (25)$$

because the first term in brackets is the quantum efficiency for intersystem crossing. We see that the second term in brackets will be small at early times because $k_p < k_f$ and $k_{ISC}$ and $[T] < [S]$, and we get the expected result.

$$\frac{\epsilon_{S,\lambda}}{\epsilon_{T,\lambda}} = \Phi_{ISC} \qquad \text{(early times, isosbestic } \lambda) \qquad (26)$$

Note that the second term in eq 25 represents a loss in population *after* product (T) is formed analogous to BET in the electron-transfer case. Thus, at longer times when $[T] > [S]$, the isosbestic point will disappear.

In both the PET and ISC cases presented, the isosbestic point appeared in a region of the spectrum where no ground-state absorption occurred and where only two species had overlapping absorption. While these two conditions simplify the situation, they are not required.

## 5. Summary and Conclusions

Isosbestic points in dynamical data can be used to provide information about quantum efficiency. Shifts in frequency of the IP are often easily detectable making this method an extremely convenient *qualitative* tool even when there is limited knowledge about the species involved. Application in this work also proves the method is a reliable *quantitative* tool in systems where species parameters, such as extinction coefficients, are known. This method also has potential to be broadly applicable. Isosbestic points in time-resolved data appear in hundreds of publications in the last five years[11] with time scales ranging from minutes[18,19] in chemically induced systems to femtoseconds[20,21] in photoinduced studies. Additionally, the method should be applicable to systems with changes invoked by other stimuli, such as pressure or temperature changes,[22] or in systems with other types of signals, such as Raman or emission.[12]

**Acknowledgment.** The authors thank Mr. Ben Reeves and Dr. Charles Spangler for provision of the donors used in this investigation. This material is based upon work supported in part by the U. S. Army Research Laboratory and the U. S. Army Research Office under Grant Number DAAD19-00-1-0162. We also thank Scientific Materials Corp. for partial support of this work.

## References and Notes

(1) Gevaert, M.; Kamat, P. V. *J. Phys. Chem.* **1992**, *96*, 9883.
(2) Palit, D. K.; Ghosh, H. N.; Pal, H.; Sapre, A. V.; Mittal, J. P.; Seshadri, R.; Rao, C. N. R. *Chem. Phys. Lett.* **1992**, *198*, 113.
(3) Wintgens, V.; Valat, P.; Garnier, F. *J. Phys. Chem.* **1994**, *98*, 228.
(4) Kovalenko, S. A.; Ernsting, N. P.; Ruthmann, J. *Chem. Phys. Lett.* **1996**, *258*, 445.
(5) Manoj, N.; Gopidas, K. R. *J. Photochem. Photobiol. A* **1999**, *127*, 31.
(6) Fukuzumi, S.; Itoh, S.; Komori, T. *J. Am. Chem. Soc.* **2000**, *122*, 8435.
(7) Kovalenko, S. A.; Ruthmann, J.; Ernsting, N. P. *Chem. Phys. Lett.* **1997**, *271*, 40.
(8) Kovalenko, S. A.; Ruthmann, J.; Ernsting, N. P. *J. Chem. Phys.* **1998**, *109*, 1894.
(9) Plaza, P.; Laage, D.; Martin, M. M. P.; Alain, V.; Blanchard-Desce, M.; Thompson, W. H.; Hynes, J. T. *J. Phys. Chem. A* **2000**, *104*, 2396.
(10) Minyung, L.; Ok Keun, S.; Jung Chul, S.; Dongho, K.; Yung Doug, S.; Seung Min, J.; Seong Keun, K. *Chem. Phys. Lett.* **1992**, *196*, 325.

(11) Full text electronic searches on the terms "isosbestic" and "transient absorption" or "photoinduced absorption" in *J. Phys. Chem. A, J. Phys. Chem. B, Chem. Phys. Lett., Chem. Phys., J. Chem. Phys., J. Photochem. Photobiol. A, J. Photochem. Photobiol. B,* and *J. Am. Chem. Soc.* returned over 400 hits, none of which contained an analytical treatment or a reference to one.

(12) Koti, A. S. R.; Krishna, M. M. G.; Periasamy, N. *J. Phys. Chem. A* **2001**, *105*, 1767.

(13) Tanigaki, K.; Ebbesen, T. W.; Kuroshima, S. *Chem. Phys. Lett.* **1991**, *185*, 189.

(14) Dimitrijevic, N. M.; Kamat, P. V. *J. Phys. Chem*. **1992**, *96*, 4811.

(15) Fraelich, M. R.; Weisman, R. B. *J. Phys. Chem*. **1993**, *97*, 11145.

(16) Lawson, D. R.; Feldhein, D. L.; Foss, C. A.; Dorhout, P. K.; Elliott, C. M.; Martin, C. R.; Parkinson, B. *J. Phys. Chem*. **1992**, *96*, 7175.

(17) Han, Y.; Spangler, L. H. *J. Phys. Chem. A*, in press.

(18) Shi, T.; Rabenstein, D. L. *J. Org. Chem. B* **1999**, *64*, 4590.

(19) Pina, F.; Melo, M. J.; Maestri, M. *J. Am. Chem. Soc.* **1997**, *119*, 5556.

(20) Vulto, S. I. E.; Kennis, J. T. M.; Streltsov, A. M. *J. Phys. Chem. B* **1999**, *103*, 878.

(21) Antipin, S. A.; Petrukhin, A. N.; Gostev, F. E.; Marevtsev, V. S.; Titov, A. A.; Barachevsky, V. A.; Strokach Yu, P.; Sarkisov, O. M. *Chem. Phys. Lett.* **2000**, *331*, 378.

(22) Robinson, G. W.; Chul Hee, C.; Urquidi, J. *J. Chem. Phys.* **1999**, *111*, 698.